Powder Technology 300 (2016) 61–72

Contents lists available at ScienceDirect

Powder Technology

journal homepage: www.elsevier.com/locate/powtec

Fluidized-bed melt granulation: Coating and agglomeration kinetics and growth regime prediction

Marta P. Villa, Diego E. Bertín, Ivana M. Cotabarren, Juliana Piña, Verónica Bucalá *

Departamento de Ingeniería Química (Universidad Nacional del Sur) and Planta Piloto de Ingeniería Química (UNS-CONICET), Camino La Carrindanga Km. 7, 8000 Bahía Blanca, Argentina

ARTICLE INFO

Article history:
Received 29 September 2015
Received in revised form 14 May 2016
Accepted 2 June 2016
Available online 3 June 2016

Keywords:
Melt granulation
Fluidized-bed
Urea
Coating
Agglomeration

ABSTRACT

Mass and population balance equations are used to describe the spray-on melt granulation process in a batch fluidized bed where coating and agglomeration can occur simultaneously. Two different models are considered to describe the agglomeration kinetics: the Equipartition Kinetic Energy (EKE) and Size Independent (SI) kernels, while the coating kinetics is represented by a power law. Based on experimental data obtained under different operating conditions (melt and air atomization flowrates, air fluidization velocity, seed diameter and bed temperature), the coating and agglomeration kinetic parameters are fitted to correctly predict the final particle size distributions. It is concluded that the SI kernel and the zero-order coating kinetics best describe the agglomeration and coating mechanisms, respectively. A correlation to predict the SI kernel from macroscopic variables and properties of the system is proposed. This tool can be used to provide starting kernel factors for solving the PBEs governing spray-on melt granulation in fluidized-bed granulators. Finally, a criterion to predict the limit of agglomeration occurrence is formulated. The criterion, which is developed in terms of dimensionless numbers that depend on process conditions and take into account mass, heat and momentum transfer phenomena, is found to be appropriate to predict the growth regime for fluidized-bed spray-on melt granulation of urea (i.e., the specific studied system).

1. Introduction

Granulation processes are considered as one of the most significant advances in the particulate product industries, providing particles with well-defined properties to meet specific end-use requirements. When liquid binders are used, granulation is classified into wet or melt processes. In wet granulation, the liquid binder is distributed on the seeds and, subsequently, the granules are dried to evaporate the solvent. In melt granulation, powders are enlarged by using meltable materials. These last binders are added to the system either as: 1) powders that melt during the granulation process or 2) atomized molten liquids [1]. The first melt granulation technique is usually called co-melt or in situ melt granulation [2], while the second method could be referred as spray-on melt granulation [3].

When liquid binders are used, the production of granules requires seeds, the binder agent and mixing. One of the major industrial equipment is the fluidized-bed granulator, wherein the liquid binder is sprayed onto the seeds and the agitation is provided by the fluidization air. Nowadays, research in melt granulation has gained interest over wet granulation for materials incompatible with water because it completely avoids the use of solvents [2,4].

The mechanisms by which size enlargement takes place are coating and/or agglomeration. Coating is the gradual growth of particles due to the deposition and solidification of liquid binder droplets on their surfaces, while agglomeration is the sticking together of two or more particles to give a larger solid particle called agglomerate [5]. Depending on the granule end-use properties, either coating or agglomeration may be preferred. Therefore, the understanding of the mechanisms prevailing in the granulation process is a prerequisite for obtaining proper control over product characteristics [6].

For wet granulation processes, many authors have studied the influence of important operating variables and physicochemical properties of the seeds and binder on the growth mechanisms in fluidized-bed granulators [7–13]. Regarding melt granulation, Abberger et al. [4], Boerefijin and Hounslow [6], Seo et al. [14] and Tan et al. [15] focused on the effect of binder spray rate, droplet size, seed size, bed temperature, atomization air pressure and fluidization air velocity on the performance of fluidized-bed spray-on melt granulation. These studies were mainly based on polyethylene glycol (PEG) or Poloxamer as model binder and glass ballotini or lactose as seeds. In addition, all these processes involved seeds of very small size, similar to or even smaller than the sprayed binder droplets. For this reason, the particles preferentially grew by agglomeration, being negligible the growth by pure coating. Recently, for urea granulation, Veliz Moraga et al. [16] studied the impact of seed size, bed temperature, binder (molten urea) flowrate,

* Corresponding author.
E-mail address: vbucala@plapiqui.edu.ar (V. Bucalá).

http://dx.doi.org/10.1016/j.powtec.2016.06.006
0032-5910/

Nomenclature

A	aggregates product mass fraction (%)
A_{LS}	deposited droplet liquid-solid interface (m^2)
A_{spray}	spray-on foot print area of the nozzle onto the particles bed (m^2)
Ap	particle surface area (m^2)
cp_u	urea mass heat capacity (J/kg K)
cp_w	water mass heat capacity (J/kg K)
c_1	fitting parameters (–)
c_2	fitting parameters (–)
c_3	fitting parameters (–)
$c_0^{'}$	fitting parameters (–)
$c_4^{'}$	fitting parameters (–)
$c_5^{'}$	fitting parameters (–)
$c_6^{'}$	fitting parameters (–)
C_{1i}	parameter for the linear approximation in Eq. (9) (m^{-2})
C_{2i}	parameter for the linear approximation in Eq. (10) (m^{-1})
D_{bot}	granulator bottom diameter (cm)
d_d	droplet arithmetic mass mean diameter (m)
d_{LS}	spread liquid droplet diameter (m)
$d_{n,g}$	gas nozzle orifice diameter (m)
$d_{n,L}$	liquid nozzle orifice diameter (m)
D_{pi}	lower node in class i (m)
$D_{p_i}^A$	average diameter of size born by aggregation (m)
d_{pi}	particles size in i class (m)
DPA	dimensionless agglomeration parameter (–)
D_{spray}	nozzle distance (m)
D_{top}	granulator top diameter (cm)
d_0	seeds arithmetic mass mean diameter (m)
e	particle coefficient of restitution (–)
E	total thermal energy to be removed from the liquid layer to solidify (J)
F_i^{G+}	appearance particles rate in i class by coating (#/s)
F_i^{G-}	disappearance particles rate in i class by coating (#/s)
FN	flux number (–)
FO	optimization objective function
Fr	Froude number (–)
G	coating growth rate (m/s)
h	deposited drop height (m)
h_a	characteristic length scale of surface asperities (m)
H_{co}	granulator conical section height (cm)
H_{cy}	granulator cylindrical section height (cm)
H_i^{A+}	flow of particles born by aggregation in class i (#/s)
H_i^{A-}	flow of particles dead by aggregation in class i (#/s)
h_{melt}	thickness of the binder layer (m)
K	constant ($kg^{8.12}\ m^{8.11}/s^{8.12}\ °C^{6.47}$)
K_d	fitting parameter (–)
K_{jet}	fitting parameter (–)
k_p	particles thermal conductivity (W/m K)
L	fluidized-bed height (m)
L_{jet}	droplets spray height (m)
L_{nozzle}	nozzle height (m)
$\dot{m}_{at}$	atomization air flowrate (kg/s)
$m_{coating}$	droplet mass necessary to cover the surface of all the particles mass within the spray zone (kg)
$\dot{m}_L$	urea melt flowrate (kg/s)
m_{layer}	liquid layer mass (kg)
m_p	particles mass holdup (kg)
m_{S0}	seeds mass (kg)
n	exponent associated with the distribution of coating liquid on the particulate material (–)
N_i	number of particles in i class (#)
N_i^A	aggregates number in i class (#)
N_p	total number of the particles within the spray zone (#)
N_{β_0}	dimensionless number for aggregation rate (–)
R_e	Reynolds numbers (–)
St^*	critical Stokes numbers (–)
St_v	viscous Stokes numbers (–)
t	time (s)
T_{bed}	bed temperature set-point (°C)
T_{fus}	urea fusion temperature (°C)
u	superficial fluidization air velocity (m/s)
u_{jet}	air jet velocity (m/s)
u_{mf}	seeds minimum fluidization velocity (m/s)
u_0	particles collision velocity (m/s)
w_i	particles mass fraction in class i (kg)
x_u	urea mass content (wt%)

Greek symbols

α	mass particles fraction in the spray zone (–)
α_i	PBE parameter (–)
β	aggregation kernel (1/# seg)
β_0	process operating conditions factor in aggregation kernel (formulation 1: 1/# seg; formulation 2: 1/# seg $m^{0.5}$)
γ	granulator angle (°)
ΔH_{ev}	water evaporation latent heat (J/kg)
ΔH_{fus}	urea fusion latent heat (J/kg)
θ	contact angle (–)
μ	binder viscosity (Pa s)
μ_{at}	atomization air viscosity (Pa s)
Π_1	mass transfer dimensionless number (–)
Π_2	heat transfer dimensionless number (–)
Π_3	momentum transfer dimensionless number (–)
ρ_{at}	atomization air density (kg/m^3)
ρ_L	binder density (kg/m^3)
ρ_p	particles density (kg/m^3)
τ_{dep}	deposition time (s)
τ_{sol}	solidification time (s)
ϕ	particles size functionality in aggregation kernel (formulation 1: (–); formulation 2: $m^{0.5}$)

Subscripts

i	class of the discrete PSD
j	class of the discrete PSD
k	class of the discrete PSD

mization air flowrates on process parameters (mass balance closure, fines deposited on granulator walls, and granulation efficiency) as well as on product properties (among others, particle size distribution, percentage of particles effectively coated or agglomerated and granule crushing strength) in order to distinguish the operating regions to avoid lump formation since coating is the preferred size-enlargement mechanism for urea production.

Two approaches have been reported to predict the growth regime in fluidized-bed granulation: a) the use of the Population Balance Equation (PBE) coupled with kinetics of particle-size change, and b) models based on dimensionless numbers.

The PBE is a mathematical description that allows to track, for example, the evolution of the particle size distributions (PSDs) of a batch system as a function of time [17]. To quantify the occurrence of agglomeration, the corresponding kinetics is required. The agglomeration parameter denoted as "kernel" (β) is a measure of the frequency of successful sticking after collision between two particles [18]. This parameter is often written as the product of two factors [6]: one depending on the process operating variables and material properties (known

as the agglomeration rate constant; β_0), and other providing the dependency of the agglomeration rate on the sizes of the particles that collide (ϕ). The determination from experimental data of the dependency of the kernel on the particle size is a complex and difficult task [19].

Regarding the ϕ models, the simplest one postulates a particle size independent kernel, based on a random agglomeration process [5]. Adetayo and Ennis [18] proposed $\phi = 1$, however they considered that only collisions of particles smaller than a critical value are successful. Moreover, several kernel models have been proposed to evaluate the effect of the particle size on the growth behavior [5,8,19]. As for the parameter β_0, it has to be fitted by using plant or laboratory granulation data [19]. Even though there are models of β_0 based on macroscopic and/or microscopic properties of the system, this parameter is also strongly dependent on the granulation system [18,20].

To take into account the particle size enlargement by coating, the PBE requires a growth rate model. The coating rate (G) is defined as the rate of increase in particle diameter due to the deposition of the liquid droplets on the particle surface, and is associated with the amount of coating material entering the system and its distribution on the particles. It is common to assume that the particles within different interval sizes grow proportional to their fractional surface area [21]. This assumption is consistent with a pattern of perfect mixing within the granulator and leads to a coating rate independent of the particle size. However, deviations from perfect mixing usually give different coating rates [22].

On the other hand, some models based on dimensionless number have been reported in the open literature to predict the prevailing growth mechanism. The paper published by Ennis et al. [23] for wet granulation was undoubtedly a major turning point. This contribution proposed a criterion to predict the occurrence of agglomeration by comparing the viscous dissipation of the binder layer to the initial kinetic energy of the two colliding particles. Besides, Akkermans et al. [24] introduced another dimensionless number, which was derived for the production of detergents in top-spray fluidized-bed granulators. This number, known as the "Flux Number" (*FN*), describes the balance between the solids flux in the spray zone and the spray flux that wets

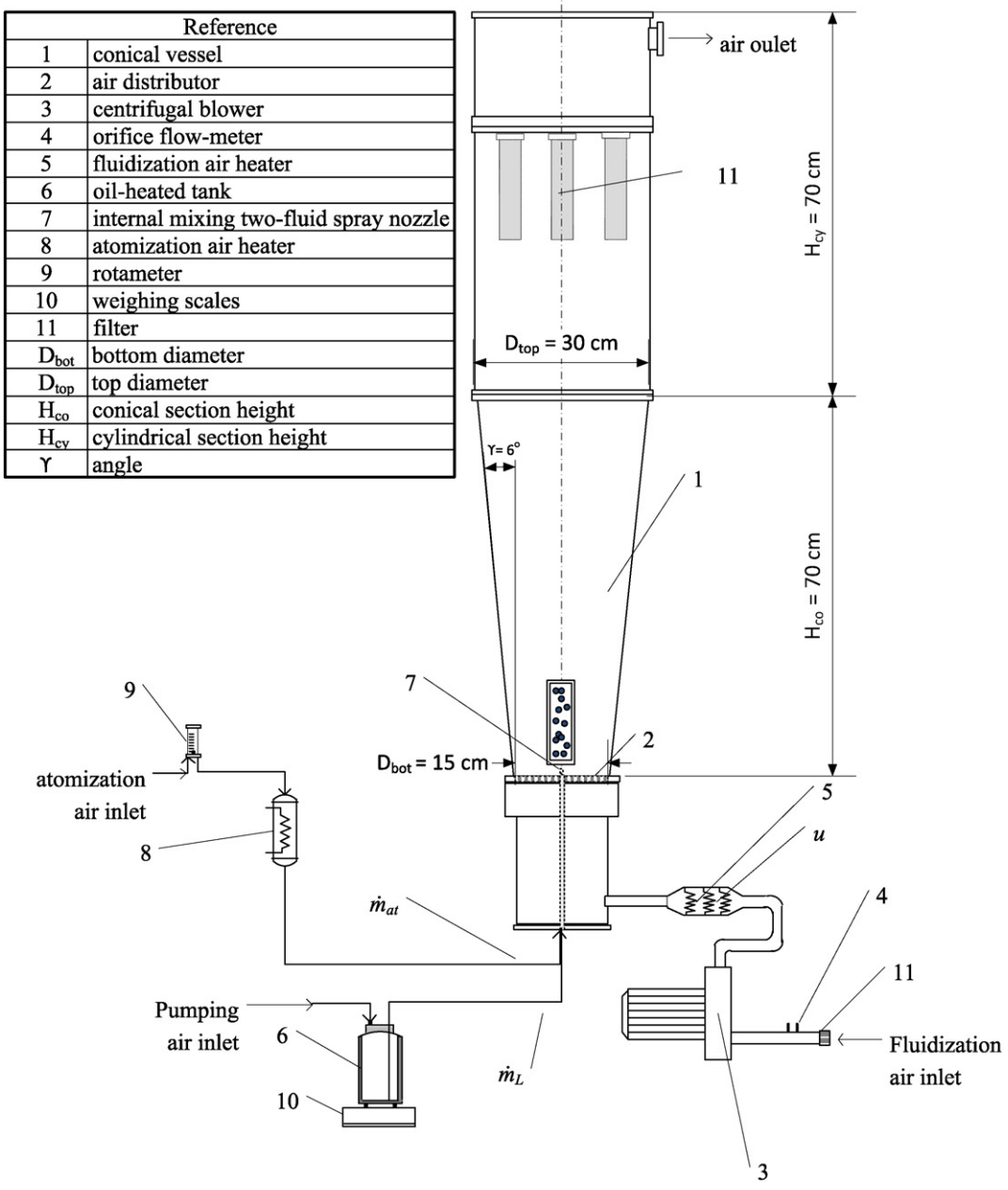

Fig. 1. Schematic representation of the batch fluidized-bed granulation unit.

the solids [6]. Although these criteria based on dimensionless numbers would be useful to predict whether agglomeration will be substantial or negligible for different granulating systems and/or materials, they do not address the tendency of agglomeration quantitatively.

Therefore, both approaches (PBE and models based on dimensionless numbers) have strengths and weaknesses.

The present work attempts to, for spray-on melt granulation processes where coating and agglomeration can occur simultaneously, predict (in terms of macroscopic variables) the final PSDs in a batch granulator and the limit between pure coating and agglomeration/coating growth regimes. Firstly, a mathematical model comprising mass and population balance equations is proposed to describe the urea granulation process in a fluidized bed. For different operating conditions (melt and air atomization flowrates, air fluidization velocity, seed diameter and bed temperature), the coating and agglomeration kinetic parameters are established to correctly predict the final particle size distribution of granular urea. Afterwards, and in order to establish a criterion to predict the limit of agglomeration occurrence without solving the PBE, a dimensionless analysis is developed. The criterion is formulated in terms of dimensionless numbers that are a function of process conditions. The proposed criterion, which takes into account mass, heat and momentum transfer phenomena, is found to be a valuable tool to predict the growth regime for fluidized-bed spray-on melt granulation.

2. Experimental procedure and data

Veliz Moraga et al. [16] reported experimental data related to urea granulation in a fluidized-bed spray-on melt granulator (see Fig. 1). The unit was constituted by a stainless steel bottom conical vessel (1), a stainless steel perforated plate as air distributor (2), a centrifugal blower (3) to provide the fluidization air. Before entering the bed, the fluidization air flowrate was measured by an orifice flow-meter (4) and preheated by an electrical heater (5) to maintain the bed temperature at the desired value. The binder (urea melt) was prepared in an oil-heated tank (6) by typically adding 1 kg of urea and a very small volume of water to reach a typical concentration value (96 wt.%). The urea melt tank was kept at a temperature close to the urea melting point (132 °C). The urea melt was delivered to an internal mixing two-fluid spray nozzle (7), located just above the air distributor, by using atomization air preheated up (8) to around 132 °C. This configuration was selected to emulate the bottom-spray system commonly used in the industry to produce granular urea [25]. The atomization air flowrate was controlled and measured by a valve and a rotameter (9), respectively.

For each run, 2 kg of urea seeds were initially charged into the granulator. To characterize the PSDs, a series of ASTM standard sieves was employed. For each experiment, the seed size distributions were narrow and obtained by sieving commercial urea particles through two contiguous ASTM sieves with a $2^{1/4}$ geometric ratio [16]. In all experiments, about 3 kg of granulated product were obtained. The PSD of the final product was determined by sieving. For each experiment, the mass fraction of agglomerates A(%) in the product was precisely measured. According to Veliz Moraga et al. [16], the total mass of agglomerates was quantified from sieves containing either only agglomerated particles or pure coated particles and small agglomerates. For the last case, a riffle splitter was used to subdivide the retained mass and the agglomerates were recognized by visual inspection and measured by weighting.

In order to determine the effect of different operating variables and seed properties on the growth mechanisms, 43 experiments were performed. To this end, the superficial fluidization air velocity (u) at bed temperature was varied from 2.76 to 5.68 m/s, the arithmetic mass mean diameter of the urea seeds (d_0) from 1.55×10^{-3} to 3.68×10^{-3} m, the urea melt flowrate ($\dot{m}_L$) from 4×10^{-3} to 1.74×10^{-4} kg/s, the bed temperature set-point (T_{bed}) from 90 to 110 °C, and the atomization air flowrate ($\dot{m}_{at}$) from 4.17 to 6.67×10^{-4} m^3/s [16]. The experiments were carried out by duplicate, except those where the binder flowrate was disturbed. This is due to the pneumatic method employed to deliver the urea melt that did not allow to obtain exactly the same melt flowrate.

3. Mathematical model

To predict the product PSDs experimentally obtained [16], the following mass and population balance equations were used:

3.1. Urea mass balance

$$\frac{dm_p}{dt} = \dot{m}_L x_u \tag{1}$$

where m_p, $\dot{m}_L$ and x_u represent the mass holdup, the melt flowrate and the urea mass content, respectively.

3.2. Population balance

In this paper the PBE formulation given by Bertin et al. [22] is used. The developed technique involves a discretization step that divides the entire domain of particle size into classes, where each class i corresponds to the interval $[D_{pi}, D_{pi+1}]$, and focuses on the accurate prediction of the number of particles in each class, N_i, and the corresponding particle size, d_{pi}, by exactly preserving the total number and mass balances (details about this method can be found in Bertin et al. [22]).

According to Bertin et al. [22] the discretized PBE for a perfectly-mixed batch process with simultaneous growth and agglomeration is:

$$\frac{dN_i}{dt} = F_i^{G+} - F_i^{G-} + H_i^{A+} - H_i^{A-} \tag{2}$$

where t is the time, F_i^{G+} and F_i^{G-} represent the rate of appearance and disappearance of particles in class i by differential growth (i.e. coating) and H_i^{A+} and H_i^{A-} describe the rate of appearance and disappearance of particles in class i by agglomeration, respectively.

The particles number in each class corresponds to a representative size, which is updated as particles appear and disappear into/from the class and is calculated as:

$$\frac{dd_{p_i}}{dt} = G(d_{p_i}) + \frac{d_{p_i}^{-2}}{3N_i}\left[F_i^{G+}\left(D_{p_i}{}^3 - d_{p_i}{}^3\right) - F_i^{G-}\left(D_{p_{i+1}}{}^3 - d_{p_i}{}^3\right) + H_i^{A+}\left(D_{p_i}^{A\,3} - d_{p_i}{}^3\right)\right] \tag{3}$$

where G is the growth rate by coating and $D_{p_i}^A$ is the average size of the particles born by agglomeration in class i [22]. F_i^{G+}, F_i^{G-}, H_i^{A+} and H_i^{A-} are calculated as:

$$F_i^{G+} = \alpha_{i-1} G(D_{p_i})\left(C_{1i-1} D_{p_i} + C_{2i-1}\right) \tag{4}$$

$$F_i^{G-} = \alpha_i G\left(D_{p_{i+1}}\right)\left(C_{1i} D_{p_{i+1}} + C_{2i}\right) \tag{5}$$

$$H_i^{A+} = \frac{1}{2}\sum_j \sum_{k/(j,k\to i)} \beta\left(d_{p_j}, d_{p_k}\right) N_j N_k \tag{6}$$

$$H_i^{A-} = N_i \sum_j \beta\left(d_{p_j}, d_{p_k}\right) N_j \tag{7}$$

where $\beta(d_{pj}, d_{pk})$ is called the agglomeration kernel and describes the frequency of agglomeration between a particle of size d_{pj} and another one of size d_{pk}. $\beta(d_{pj}, d_{pk})$ provides the dependency of the agglomeration rate on the operating conditions and the particle size and physical

properties [26,27]. In Equation 6, the notation $k/(j,k\rightarrow i)$ means: all classes k such that agglomeration between particles of classes j and k generate a particle of class i. C_{1i}, C_{2i} and α_i are calculated as:

$$\alpha_i = \begin{cases} 1 & if\left(C_{1i}D_{p_{i+1}} + C_{2i}\right) > 0 \\ 0 & if\left(C_{1i}D_{p_{i+1}} + C_{2i}\right) \le 0 \end{cases} \tag{8}$$

$$C_{1i} = \frac{\frac{{D_{p_{i+1}}}^4 - {D_{p_i}}^4}{D_{p_{i+1}} - D_{p_i}} - 4{d_{p_i}}^3}{\frac{1}{2}\left(D_{p_{i+1}} + D_{p_i}\right)\left({D_{p_{i+1}}}^4 - {D_{p_i}}^4\right) - \frac{4}{5}\left({D_{p_{i+1}}}^5 - {D_{p_i}}^5\right)} N_i \tag{9}$$

$$C_{2i} = \frac{N_i - \frac{C_{1i}}{2}\left({D_{p_{i+1}}}^2 - {D_{p_i}}^2\right)}{D_{p_{i+1}} - D_{p_i}} \tag{10}$$

Following the development of Kumar et al. [28], the average size of all newborn particles by agglomeration in class i is calculated by dividing the total newborn particle volume by the total newborn particle number:

$$D^A_{p_i} = \left[\frac{\sum_j \sum_{k/(j,k\rightarrow i)} \beta\left(d_{p_j}, d_{p_k}\right) N_j N_k \left({d_{p_j}}^3 + {d_{p_k}}^3\right)}{\sum_j \sum_{k/(j,k\rightarrow i)} \beta\left(d_{p_j}, d_{p_k}\right) N_j N_k}\right]^{\frac{1}{3}} \tag{11}$$

3.3. Coating and agglomeration kinetics

A common practice is to assume that particles belonging to different interval sizes grow proportional to its fractional surface area [29]. This assumption is consistent with a pattern of perfect mixing in the granulator and leads to a coating rate that is independent of particle size. However, deviations from perfect mixing may lead to a different coating rate. Therefore, in this paper, a coating rate described by the power law is proposed [22]:

$$G(d_p) = \frac{2\dot{m}_L x_u}{\pi \rho_p \sum_i N_i {d_{p_i}}^{2+n}} {d_p}^n \tag{12}$$

If $n = 0$, the coating rate is independent of particle size and all particles grow by coating at the same rate; if aggregation does not take place, the final PSD maintains its initial shape. If $n > 0$, the larger particles grow faster than smaller ones, causing a final PSD wider than the initial one. Finally, if $n < 0$, the smaller particles grow faster than larger ones, and the final PSD results narrower than the initial one.

As suggested by several authors [30,31] and as afore-mentioned, the agglomeration kernel can be represented by two factors: one depending exclusively on the particle size (ϕ) and the other on the process operating conditions (β_0):

$$\beta\left(d_{p_j}, d_{p_k}\right) = \beta_0\, \phi\left(d_{p_j}, d_{p_k}\right) \tag{13}$$

In this paper, two different formulations are proposed: 1) β is considered independent of the size of the particles that collide (i.e., $\phi = 1$) and 2) ϕ is represented by the equipartition kinetic energy coalescence model (EKE model), which provides a theoretical basis for the collision frequency of particles in fluidized beds [32]:

$$\phi\left(d_{p_j}, d_{p_k}\right) = \left(d_{p_j} + d_{p_k}\right)^2 \sqrt{\frac{1}{{d_{p_j}}^3} + \frac{1}{{d_{p_k}}^3}} \tag{14}$$

3.4. Agglomerate mass fraction in the granular product

Eqs. (2) and (3) do not allow to numerically quantify the mass of the agglomerates. To this end a new equation is required:

$$\frac{dN^A_i}{dt} = H^{A+}_i - H^{A-}_i \frac{N^A_i}{N_i} + F^{G+}_i \frac{N^A_{i-1}}{N_{i-1}} - F^{G-}_i \frac{N^A_i}{N_i} \tag{15}$$

In Eq. (15), the first term of the right-hand side is the number of particles born by agglomeration in class i while the second one represents the total particle number leaving class i by agglomeration, multiplied by the number fraction of agglomerates in class i. Analogously, the third and fourth term of the right-hand side in Eq. (15) describe the number flow of agglomerates growing into class i from class $(i-1)$ and growing out of class i into class $(i+1)$ by coating, respectively.

The agglomerate mass fraction is calculated as:

$$A = \frac{\sum_i N^A_i {d_{p_i}}^3}{\sum_i N_i {d_{p_i}}^3} \tag{16}$$

The model code is implemented in FORTRAN programming language. By means of a Gear subroutine, the set of ordinary differential Eqs. (1)–(3) and (15) is integrated to estimate the particle mass, total particle number, mean size and agglomerate number in each class. Then, the set of algebraic equations that allows predicting the coating and agglomeration rates (Eqs. (12)–(14)) and the agglomerate mass fraction (Eq. (16)) is solved.

Simulations for the 43 experimental points were performed, and a least square optimization scheme was implemented to fit the two kinetics parameters: the exponent of the power law that describes the coating rate (Eq. (12)) and the factor β_0 of the agglomeration rate (Eq. (13)). Each experimental point was simulated twice, once for each agglomeration kinetics ($\phi = 1$ and ϕ given by Eq. (14)).

Considering that: a) the granulometry of urea particles is available as weight % (i.e., the experimental data were obtained by sieving [16]) instead of number PSDs, and b) the PSDs should be represented by the density function because the discretization grid has classes of different interval width, the optimization objective function for the fitting procedure is defined as follows:

$$FO = \min_{p,\beta_0} \sum_i \left(\frac{w_i|_{Calculated} - w_i|_{Experimental}}{D_{p_{i+1}} - D_{p_i}}\right)^2 \tag{17}$$

where w_i is the weight fraction of particles in class i. The calculated weight fractions are determined, based on the particle number in each class obtained from the PBE solution, as follows:

$$w_i|_{Calculated} = \frac{N_i {d_{p_i}}^3}{\sum_i N_i {d_{p_i}}^3} \tag{18}$$

Besides, the optimization is subjected to the following constraint: the calculated agglomerate mass fraction in the granular product has to be equal to the experimental value.

4. Model results and discussion

4.1. PBE results

For each experiment, the best n and β_0 values were obtained by minimizing Eq. (17). The best n values varied between −0.05 and 0.12, being the average value for the 43 experiments $n = 0.05$. This result suggests a coating kinetics almost independent of the particle size.

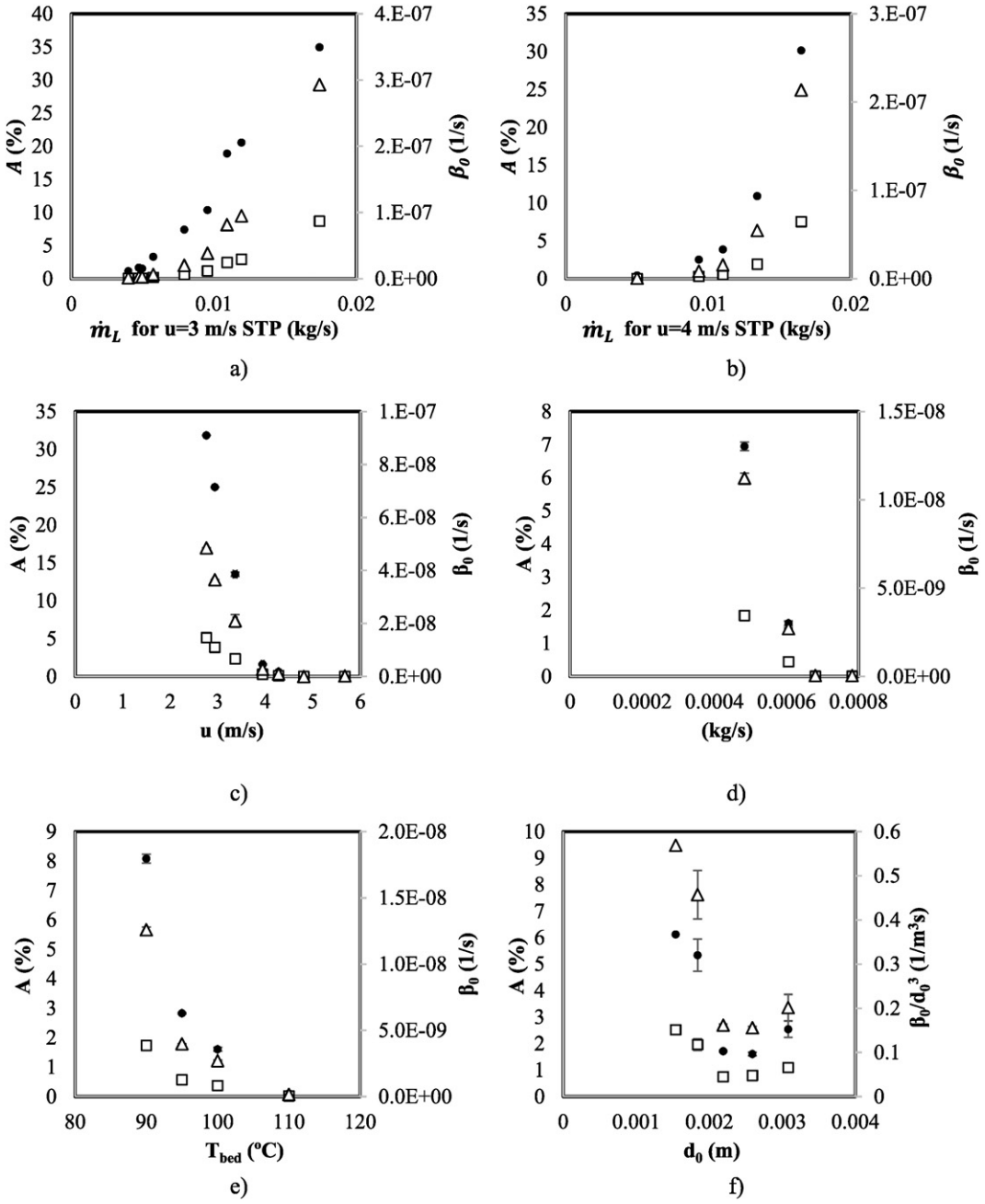

Fig. 2. Agglomerate mass percentage (●) and agglomeration kernel (□: $\phi = 1$; Δ: EKE model) as a function of the operating variables: a) urea melt flowrate for $u = 3$ m/s STP, b) urea melt flowrate for $u = 4$ m/s STP, c) superficial fluidization air velocity at bed temperature, d) atomization air flowrate, e) bed temperature set-point and f) arithmetic mass mean diameter of the seeds.

Fig. 2 presents the experimental agglomerate mass fraction $A(\%)$ and the optimal β_0 factors (obtained, for each experiment and kernel model; according to the above described fitting procedure) as a function of the studied operating variables.

The agglomerate mass percentage increases as the binder flowrate increases and the fluidization air velocity, atomization air flowrate and bed temperature decrease (details about the effect of the operating variables and granule properties on the occurrence of agglomeration can be found in Veliz Moraga et al. [16]). For both agglomeration kinetics (Section 3.3), the factor β_0 exhibits the same trends than the ones found for the agglomerate mass fraction (Fig. 2.a–e). The trend exhibited by $A(\%)$,as a function of the seed arithmetic mean size, is followed by the variable $\beta_0/{d_0}^3$ instead of β_0 (Fig. 2.f). This is in good agreement with the fact that the mass of agglomerated particles is proportional to the mass of the particles that collide and to $\beta_0/{d_0}^3$. Considering this representation, the agglomerate mass fraction and the kernel factors show both a non-monotonic behavior against the seed size, this behavior is discussed elsewhere [16].

Fig. 3 shows the experimental and calculated (by using the best fitted β_0 factors for each agglomeration kernel model) mass PSDs for three selected representative experiments. In the same figure, the seed size range used in each experiment is indicated. As expected, the product PSD shift towards particle sizes bigger than the seeds. The results indicate that the prediction of the experimental PSDs is quite similar by using both agglomeration kinetic models. However, since the kernel models are different, different β_0 optimal values are found for each model. Indeed, for 95% of the experiments, the obtained R^2 was higher than 0.8.

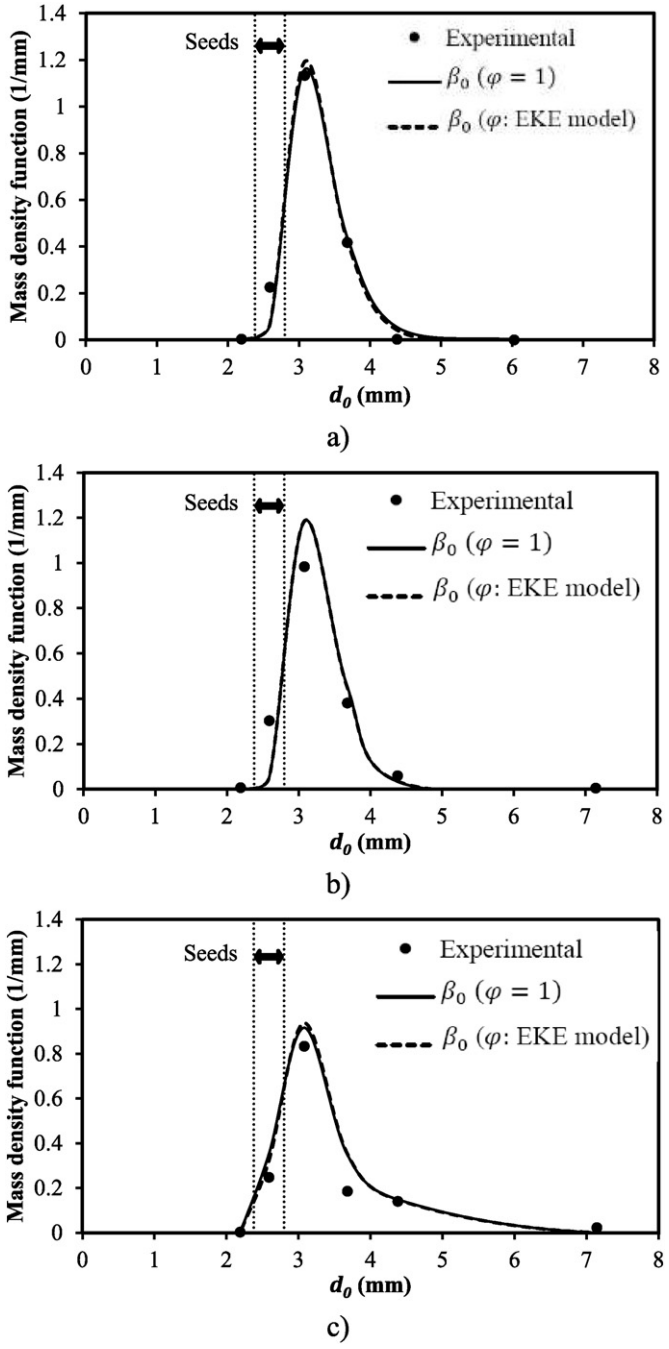

Fig. 3. Experimental and calculated PSD for a) $\dot{m}_L = 4 \times 10^{-3}$ kg/s ($A(\%) = 1.15$), b) $\dot{m}_L = 9.5 \times 10^{-3}$ kg/s ($A(\%) = 10.4$) and c) $\dot{m}_L = 1.74 \times 10^{-2}$ kg/s ($A(\%) = 35$).

Considering that the results are similar for both tested agglomeration kinetics, the simplest model (i.e., $\phi = 1$) is chosen to simulate the urea melt granulation process.

4.2. Semi-empirical correlation to predict the agglomeration kernel

For melt granulation, Tan et al. [33] indicated that the agglomeration kernel depends on various factors, such as particle wettability, particle velocity, binder type and concentration. Chua et al. [34] suggested that there are four major events occurring at the granule level that influence β_0: droplet-particle collisions, particle-particle collisions, droplet spreading and droplet solidification. The time scale of the liquid solidification was the largest of the four proposed events, indicating that the solidification rate has great influence on the agglomeration occurrence.

The bed temperature is directly related to the binder solidification rate, therefore it significantly influences the agglomeration kinetics [35]. The binder solidification rate can be calculated from an energy balance at the droplet-particle interface [15].

Regarding the interparticle and droplet-particle collisions, the movement of particles and droplets within the fluidized bed is mainly determined by the fluidization gas velocity. Higher fluidization velocities tend to reduce the agglomeration rate due to higher probability of particle rebound, as a consequence of an increased impact kinetic energy and more agitation that favors the breakage of liquid bridges [36].

Based on the above considerations, a semi-empirical correlation is proposed to relate β_0 with the process operating conditions. To this end, the following hypotheses are considered:

1) The β_0 behavior depends on three dimensionless numbers. These numbers are related to operating conditions and properties of the binder and seeds, i.e. a macroscopic approach is chosen. The first dimensionless number relates the characteristic times of the droplet deposition and the binder solidification. The second one describes the thermal phenomena of the solidifying droplet, while the third one is associated to the movement of particles within the fluidized bed.
2) At each instant, according to Chua et al. [37], a fraction α of the particle population is being wetted by the droplets (i.e., there is a spray active zone within the granulator).
3) The urea solidification occurs at the droplet/particle interface.
4) The water evaporation occurs at the droplet/gas interface.
5) The particle temperature is equal to the overall bed temperature [38].
6) The mean seed particle diameter is used to evaluate the dimensionless numbers since this variable is a priori known.

Based on the above assumptions, the following dimensionless numbers are proposed:

4.2.1. Mass transfer dimensionless number

The droplet mass necessary to completely coat all the particles in the spray zone can be calculated as:

Particle number in the spray zone
× Droplet number that cover the surface of one particle
× Mass of a binder single droplet

The particle number (Np) within the spray zone is calculated as:

$$Np = \frac{\alpha\, m_{S0}}{\rho_p \frac{\pi}{6} {d_0}^3} \tag{19}$$

where m_{S0} is the seed mass, α is the mass fraction of particles in the spray zone and d_0 is the seed arithmetic mean diameter. The droplet number necessary to completely coat one single particle can be calculated as the ratio between the surface area of one particle (Ap) and the contact area of a deposited droplet at the liquid-solid interface (A_{LS}):

$$\frac{Ap}{A_{LS}} = \frac{\pi {d_0}^2}{\frac{\pi}{4} {d_{LS}}^2} = \frac{4 {d_0}^2}{{d_{LS}}^2} \tag{20}$$

where d_{LS} is the diameter of the spread liquid droplet. According to Clarke et al. [39] and Chua et al. [34], d_{LS} can be estimated as a function of the droplet size d_d and the contact angle θ:

$$d_{LS} = f(\theta) d_d = \left[\frac{4\, sin(\theta)^3}{2 - 3\, cos(\theta) + cos(\theta)^3} \right]^{\frac{1}{3}} d_d \tag{21}$$

Taking into account Eqs. (20) and (21), the droplet mass necessary to form a liquid layer onto the surface of one particle is:

$$m_{layer} = \frac{4{d_0}^2}{f(\theta)^2 {d_d}^2}\rho_L \frac{\pi}{6}{d_d}^3 = \frac{2\pi\rho_L {d_0}^2 d_d}{3f(\theta)^2} \tag{22}$$

By multiplying Eq. (22) by Eq. (19), the droplet mass necessary to cover the surface of all the particles within the spray zone is:

$$m_{coating} = Np\, m_{layer} = \frac{4\rho_L \alpha\, m_{S0} d_d}{\rho_p d_0 f(\theta)^2} \tag{23}$$

Hence, the characteristic time for droplet deposition is defined as the droplet mass necessary to form a liquid layer onto the surface of all the particles within the spray zone (Eq. (23)) divided by the melt flowrate:

$$\tau_{dep} = \frac{\frac{4\rho_L \alpha\, m_{S0} d_d}{\rho_p d_0 f(\theta)^2}}{\dot{m}_L} = \frac{4\rho_L \alpha\, m_{S0} d_d}{\rho_p d_0 f(\theta)^2 \dot{m}_L} \tag{24}$$

On the other hand, the physical model of the solidification process has been investigated by several authors. In general, equations are proposed for a flat liquid layer with a temperature that exceeds the melting point [35,40]. Since for the available experiments [16] the liquid layer is deposited on a solid surface with a temperature below the binder melting point, a heat transfer process has to be considered. Based on the solution of the one-dimensional transient heat conduction in a semi-infinite plate [41], the urea heat balance is given by:

$$\frac{\pi}{2}{d_0}^2 \rho_p cp_u (T_{fus} - T_{bed})\sqrt{\frac{k_p \tau_{sol}}{\pi \rho_p cp_u}} = m_{layer} x_u \Delta H_{fus} \tag{25}$$

where cp_u is the urea heat capacity, T_{fus} the fusion temperature, k_p the particles thermal conductivity, x_u the urea mass content, ΔH_{fus} the latent heat of fusion and τ_{sol} is the melt solidification time.

The solidification time is then obtained by replacing Eq. (22) in Eq. (25):

$$\tau_{sol} = \frac{16\pi}{9\rho_p cp_u k_p}\left[\frac{\rho_L x_u d_d \Delta H_{fus}}{f(\theta)^2 (T_{fus} - T_{bed})}\right]^2 \tag{26}$$

Finally, the dimensionless number that compares the binder solidification and the droplet deposition characteristic times is formulated as:

$$\Pi_1 = \frac{\tau_{sol}}{\tau_{dep}} = \frac{\frac{16\pi}{9\rho_p cp_u k_p}\left[\frac{\rho_L x_u d_d \Delta H_{fus}}{f(\theta)^2 (T_{fus} - T_{bed})}\right]^2}{\frac{4\rho_L \alpha\, m_{S0} d_d}{\rho_p d_0 f(\theta)^2 \dot{m}_L}} = \frac{4\pi d_0 \rho_L \dot{m}_L d_d {x_u}^2 {\Delta H_{fus}}^2}{9 f(\theta)^2 cp_u k_p \alpha\, m_{S0} (T_{fus} - T_{bed})^2} \tag{27}$$

4.2.2. Heat transfer dimensionless number

The urea granulation process involves several thermal phenomena. In addition to the sensible heats associated to the streams that enter and leave the granulator, latent heats are present in the heat balance. A very important dimensionless number in phase change phenomena is the Stefan number, which is the ratio of sensible to latent heat [42,43]. Regarding the latent heats, the urea solidification releases a large amount of dissolution heat while the evaporation of the small amount of water present in the melt withdraws energy from the system, partially balancing the exothermic dissolution heat. The evaporation heat per mass unit is about nine times higher than the urea dissolution one.

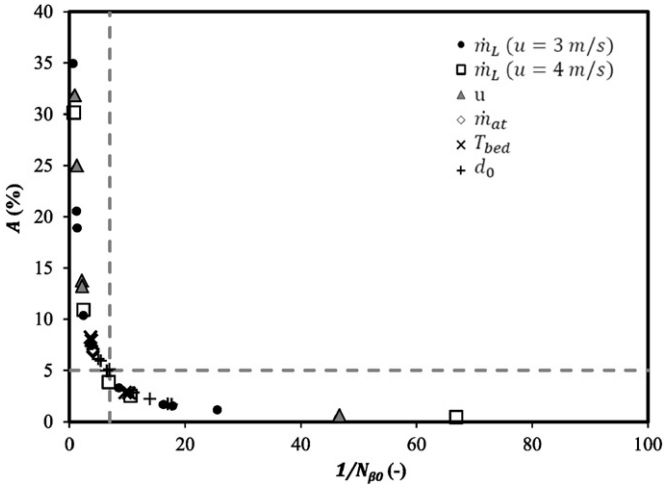

Fig. 4. Agglomerate mass percentage as a function of $1/N_{\beta_0}$ for changes in different process conditions.

Nevertheless, due to the high urea mass content (about 96 wt.%), the dissolution heat is considerably higher than the evaporation one [38]. To quantify the two latent heats involved in the urea granulation process, the Stefan number is written as:

$$\Pi_2 = \frac{[x_u cp_u + (1-x_u)cp_w](T_{fus} - T_{bed})}{x_u \Delta H_{fus} - (1-x_u)\Delta H_{ev}} \tag{28}$$

It is worth to mention that in the first dimensionless number (Π_1), just the dissolution latent heat is considered since Π_1 is based on the energy balance at the liquid layer/solid interface where only urea solidification occurs (Eq. 25).

4.2.3. Momentum transfer dimensionless number

The higher the particles velocity through the binder atomization zone, the better the distribution of molten urea on the seeds and consequently, the lower the probability of large agglomerates formation. Furthermore, higher velocities increase the disruptive forces. Thus, the third dimensionless number is defined as the ratio between the excess air velocity (i.e., the difference between the superficial air velocity and the minimum fluidization one) and the minimum fluidization velocity:

$$\Pi_3 = \frac{u - u_{mf}}{u_{mf}} \tag{29}$$

4.2.4. Dimensionless agglomeration kernel

In order to obtain a dimensionless correlation, the dimensionless number N_{β_0}, which includes the factor β_0, is proposed:

$$N_{\beta_0} = \beta_0 \frac{{m_{S0}}^2}{(\dot{m}_L x_u)\rho_p \frac{\pi}{6}{d_p}^3} \tag{30}$$

As shown in Fig. 4, the agglomerate mass percentage for all the studied variables follows a unique trend as a function of $1 / N_{\beta_0}$. Therefore, the dimensionless number given by Eq. (30) is appropriate.

Finally, the following correlation is proposed to gather the dimensionless groups defined by Eqs. (27)–(30):

$$N_{\beta_0} = c_0' {\Pi_1}^{c_1} {\Pi_2}^{c_2} {\Pi_3}^{c_3} \tag{31}$$

where c_0', c_1, c_2 and c_3 are fitting parameters. By replacing Eqs. (27)–(30)

in Eq. (31), the next expression is obtained:

$$\beta_0 \frac{{m_{S0}}^2}{(\dot{m}_L x_u)\rho_p \frac{\pi}{6}{d_p}^3} = c_0' \left[\frac{4\pi d_0 \rho_L \dot{m}_L d_d {x_u}^2 \Delta {H_{fus}}^2}{9f(\theta)^2 cp_u k_p \alpha\, m_{S0}(T_{fus}-T_{bed})^2}\right]^{c_1} \left[\frac{[x_u cp_u + (1-x_u)cp_w](T_{fus}-T_{bed})}{x_u \Delta H_{fus} - (1-x_u)\Delta H_{ev}}\right]^{c_2} \left[\frac{u-u_{mf}}{u_{mf}}\right]^{c_3} \tag{32}$$

For the calculation of the mass fraction of particles in the active zone (α), it is considered that the spray-zone height depends on the ratio between the droplets spray height (L_{jet}) and the fluidized-bed height (L). Therefore:

$$\alpha = \frac{L_{jet}}{L} \tag{33}$$

Following the work of Hong et al. [44], the dimensionless ratio of L_{jet} to the nozzle orifice diameter for the gas flow ($d_{n,g}$) is expressed as a function of the Froude and Reynolds numbers as follows:

$$\frac{L_{jet}}{d_{n,g}} = K_{jet} Fr^{c_4'} Re^{c_5'} \tag{34}$$

The Froude and Reynolds numbers are given by $Fr = \rho_{at} {u_{jet}}^2 / \rho_p g d_{n,g}$ and $Re = \rho_{at} u_{jet} d_0 / \mu_{at}$. ρ_{at} and μ_{at} are the atomization air density and viscosity, respectively, and u_{jet} is the air jet velocity. K_{jet}, c_4' and c_5' are fitting parameters. By replacing Eq. 34 in Eq. 33 and considering $u_{jet} = \frac{4\dot{m}_{at}}{\pi \rho_{at} {d_{n,g}}^2}$, the mass fraction of particles in the active zone is calculated as:

$$\alpha = \frac{K_{jet} d_{n,g} Fr^{c_4'} Re^{c_5'}}{L} = K_{jet} \frac{d_{n,g}}{L} \left(\frac{\rho_{at} {u_{jet}}^2}{\rho_p g d_{n,g}}\right)^{c_4'} \left(\frac{\rho_{at} u_{jet} d_0}{\mu_{at}}\right)^{c_5'} = K_{jet} \frac{d_{n,g}}{L} \left(\frac{16 {\dot{m}_{at}}^2}{\pi^2 \rho_{at} \rho_p g {d_{n,g}}^5}\right)^{c_4'} \left(\frac{4\dot{m}_{at} d_0}{\pi {d_{n,g}}^2 \mu_{at}}\right)^{c_5'} \tag{35}$$

To solve Eq. (32), an expression for the droplet diameter (d_d) is required. Taking into account that an important parameter to characterize the droplet diameter in twin-fluid nozzles is the gas-to-liquid mass flowrate ratio ($\dot{m}_L/\dot{m}_{at}$) [45], the ratio of d_d to the nozzle orifice diameter for the liquid flow ($d_{n,L}$) is given by:

$$\frac{d_d}{d_{n,L}} = K_d \left(\frac{\dot{m}_L}{\dot{m}_{at}}\right)^{c_6'} \tag{36}$$

where K_d and c_6' are fitting parameters.

By replacing Eqs. (35) and (36) in Eq. (32) and considering $c_4 = c_1 c_4'$, $c_5 = c_1 c_5'$, $c_6 = c_1 c_6'$ and $c_0 = c_0' \left(\frac{K_d}{K_{jet}}\right)^{c_1}$, the following correlation is obtained:

$$\frac{\beta_0 {m_{S0}}^2}{(\dot{m}_L x_u)\rho_p \frac{\pi}{6}{d_p}^3} = c_0 \left[\frac{4\pi d_0 \rho_L \dot{m}_L d_{n,L} {x_u}^2 \Delta {H_{fus}}^2 L}{9f(\theta)^2 cp_u k_p d_{n,g}\, m_{S0}(T_{fus}-T_{bed})^2}\right]^{c_1} \left[\frac{[x_u cp_u + (1-x_u)cp_w](T_{fus}-T_{bed})}{x_u \Delta H_{fus} - (1-x_u)\Delta H_{ev}}\right]^{c_2} \left[\frac{u-u_{mf}}{u_{mf}}\right]^{c_3} \left[\frac{\pi^2 \rho_{at} \rho_p g {d_{n,g}}^5}{16 {\dot{m}_{at}}^2}\right]^{c_4} \left[\frac{\pi {d_{n,g}}^2 \mu_{at}}{4\dot{m}_{at} d_0}\right]^{c_5} \left[\frac{\dot{m}_L}{\dot{m}_{at}}\right]^{c_6} \tag{37}$$

In order to correlate the kernel as a function of the studied operating conditions and seed mean size, the optimal c_k ($k = 0$–6) were found by minimizing the sum of the squared errors between the measured and predicted β_0 for the 43 available experimental points. The optimal value found for c_4 (0.00348) indicated that the term raised to the c_4 power had a negligible influence on the correlation kernel. Therefore, this term was removed from the correlation (Eq. 37) and a new multi-parameter fitting was performed. Considering the best new fitted parameters, the kernel correlation (Eq. 37) becomes:

$$\frac{\beta_0 {m_{S0}}^2}{(\dot{m}_L x_u)\rho_p \frac{\pi}{6}{d_p}^3} = 0.028 \left[\frac{4\pi d_0 \rho_L \dot{m}_L d_{n,L} {x_u}^2 \Delta {H_{fus}}^2 L}{9f(\theta)^2 cp_u k_p d_{n,g}\, m_{S0}(T_{fus}-T_{bed})^2}\right]^{0.3} \left[\frac{[x_u cp_u + (1-x_u)cp_w](T_{fus}-T_{bed})}{x_u \Delta H_{fus} - (1-x_u)\Delta H_{ev}}\right]^{1.9} \left[\frac{u-u_{mf}}{u_{mf}}\right]^{-4.6} \left[10^6 \frac{\pi {d_{n,g}}^2 \mu_{at}}{4\dot{m}_{at} d_0}\right]^{2.6} \left[\frac{\dot{m}_L}{\dot{m}_{at}}\right]^{1.2} \tag{38}$$

Eq. (38) provides a correlation to predict the kernel factor by using macroscopic variables and properties of the system. Therefore, it represents an interesting tool to solve the PBE for melt granulation in fluidized-bed granulators. It is worth to mention that all the physical properties involved in Eq. (38) (ρ_p, ρ_L, μ_{at}, cp_u, cp_w, k_p, ΔH_{fus}, ΔH_{ev}) are calculated from Meessen [46] and Incropera [52], $d_{n,g}$ and $d_{n,L}$ are the geometrical dimensions of the spray nozzle and m_{S0} and x_u are fixed values for all the experiences (2 kg and 0.96, respectively). L is experimentally determined for each test, $f(\theta)$ is considered equal to 1.83 (i.e., a typical value of $\theta = 45°$ is assumed) for all the experiments and u_{mf} is calculated by the Ergun equation [53].

5. Dimensionless number to predict the occurrence of agglomeration

Even though Eq. (38) is an interesting tool to calculate final particle size distributions in fluidized-bed melt granulators, the complexity of the PBE solution may limit its application. Instead, the development of a criterion to predict the occurrence of aggregation or coating in terms operating variables (such as the binder flowrate, fluidization air velocity, bed temperature, atomization air flowrate) and an initial particle size would be very valuable to establish a priori the granules quality.

5.1. Previous dimensionless numbers and model validation

Several attempts have been made in the past to establish a parameter that allows predicting the growth regimes in different types of granulation processes. In fact, for wet granulation, Ennis et al. [47] were the first introducing a microscopic characterization of the granulation phenomena to explain the growth mechanism. The established theory assumed that when two non-deformable particles moving at given velocities and surrounded by a thin viscous binder layer approach to each other, a subsequent formation of a dynamic liquid bridge between them occurs. Then, a collision results in successful agglomeration when the formed liquid bridge solidifies keeping both particles bonded. The Ennis theory is founded on two dimensionless numbers: the viscous (St_v) and the critical (St^*) Stokes numbers.

The St_v represents the ratio between the kinetic energy of the particle collision and the viscous dissipation caused by the dynamic liquid bridge, as follows:

$$St_v = \frac{4\rho_p d_0 u_0}{9\,\mu} \tag{39}$$

where μ is the binder viscosity and u_0 is the collision velocity. Following Wasserman et al. [48] and Hede et al. [49], u_0 was as approximated by the fluidized bed excess gas velocity ($u - u_{mf}$). Furthermore, St^* is defined as:

$$St^* = \left(1 + \frac{1}{e}\right) \ln\left(\frac{h_{melt}}{h_a}\right) \tag{40}$$

where e is the particle coefficient of restitution, h_{melt} is the thickness of the binder layer and h_a is a measurement of the particle asperity height. According to the Ennis model, if $St_v < St^*$ all collisions are successful (i.e., agglomeration occurs) whereas if $St_v > St^*$ the granules grow by coating since coalescence is not feasible.

On the other hand, Akkermans et al. [24] introduced a parameter known as "Flux Number" (FN) derived for the industrial production of detergents in top-spray fluidized-bed granulators. The FN has been particularly used by Boerefijn and coworkers [6,50] to scale melt granulation processes from batch to continuous and to model the agglomeration mechanism. As afore-mentioned, the FN describes the balance between the solids flux in the spray zone (for top-spray configurations, the binder-particle contact zone is in the upper part of the fluidized bed) and the spray flux that wets the solids [6], as follows:

$$FN = log\left[\frac{(u-u_{mf})A_{spray}\rho_p}{\dot{m}_L}\right] \quad (41)$$

where A_{spray} is the spray-on foot-print area of the nozzle onto the particles bed. This area is evaluated at the nozzle distance D_{spray} that is given by:

$$D_{spray} = L_{nozzle} - L \quad (42)$$

where L_{nozzle} is the nozzle height and L is the fluidized-bed height.

According to Akkermans' studies, $FN > 3$ ensures particles growth by pure coating. However, excessively high FN must be avoided since they cause undesirable effects such as too long operating times for low $\dot{m}_L$ in batch processes, larger equipment to achieve identical residence time in continuous processes, and elutriation of particles at very high fluidization air flowrate [49]. Furthermore, Wasserman et al. [48] used the criterion established by Akkermanns et al. [24] to determine the operating regime of a top-spray fluidized-bed granulator for detergent production, finding that coating is the main size enlargement mechanism within the range $3.5 < FN < 5$. These authors also used the viscous Stokes number as a criterion to ensure particle growth by pure coating ($St_v > 10$, preferably $100 < St_v < 1000$).

Firstly, the feasibility of using dimensionless numbers already proposed in the open literature to predict the growth mechanism of urea granules is examined. From the available experimental data, St_v and St^* are evaluated according to Eqs. (39) and (40). It should be noted that the value of the coefficient of restitution e for the urea granules is 0.35 (it represents the mean value experimentally obtained by using the apparatus and the methodology given by Khoufech et al. [51]). Besides, the mean particle asperity height h_a is established at 0.01 mm based on SEM photographs of urea particles [16]. For each experiment, the thickness of the binder layer h_{melt} is calculated considering the seed size and the binder atomized mass.

Table 1 summarizes St_v and St^* for the 43 performed experiments, which involved variations in: $(u - u_{mf})$, $\dot{m}_L$ for two different superficial fluidization air velocities, $\dot{m}_{at}$, d_0 and T_{bed}. Noticeably, in all cases it is verified that $St_v > St^*$, indicating that the dominat mechanism for granule growth is pure coating. Evidently, this result disagrees with the agglomerate mass fraction obtained in several experiments (see Fig. 2). Furthermore, the values of the viscous Stokes number are between 1447 and 2789, high above the minimum value ($St_v > 10$) reported by Wasserman et al. [48] to ensure particle growth by pure coating and even outside the preferred range $100 < St_v < 1000$ to successfully operate under a coating regime [49]. In conclusion, both criteria, the one developed by Ennis et al. [47] and that proposed by Wasserman et al. [48] based on the Stokes number, are invalid for the system under study.

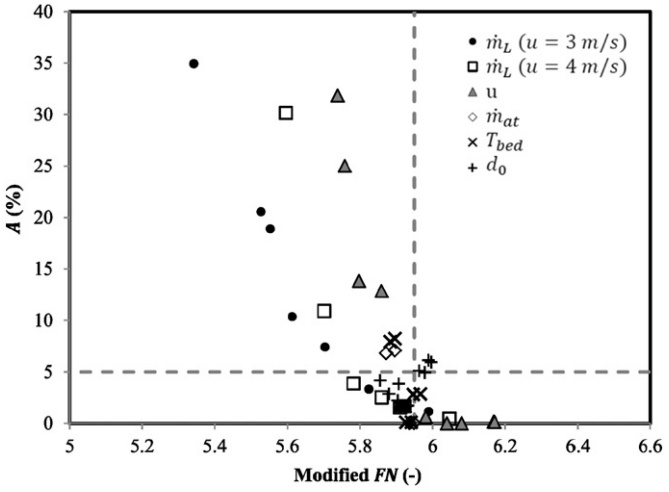

Fig. 5. Agglomerate mass fraction as a function of the modified FN for changes in different process conditions.

Similarly, the criterion of FN is analyzed. To determine this parameter through Eq. (41), it is necessary to know the spray-on foot-print area of the nozzle onto the particles bed. This variable is easily derived for top-spray fluidized-bed granulators. However, the process under study is based on a bottom-spray configuration. Hence, the binder sprayed droplets are immersed in the fluidized bed of particles, being the spray-on foot-print area not well defined. To estimate FN values representative for the urea granulation system, the value of the functional group reported by Akkermanns is modified by dividing by the spray area given in that contribution [24]. Thus, an optimum range between 5 and 7.5 is obtained for the modified FN. Then, the modified FN is calculated (Eq. (41) excluding the contact area between the binder spray and particles) for the all the experiments. The relationship between the modified FN and the mass fraction of agglomerates for each manipulated process variable is shown in Fig. 5. For urea granulation, the modified FN must be greater than 5.95 to ensure an almost pure coating regime (i.e., % A less than 5% by weight), while for the modified FN reported

Table 1
Comparison between St^* and St_v for the different performed experiments.

Process variable																
$u - u_{mf}$			$\dot{m}_L$ (u = 3 m/s)			$\dot{m}_L$ (u = 4 m/s)			$\dot{m}_{at}$			d_0			T_{bed}	
St^*	St_v		St^*	St_v		St^*	St_v		St^*	St_v		St^*	St_v		St^*	St_v
11.2	1447	10	11.0	2323	19	11.0	3320	24	10.7	2167	28	12.3	2917	38	11.0	2274
11.2	1588	11	10.7	2366	20	10.6	3284	25	10.9	2188	29	12.3	3000	39	11.0	2225
10.9	1896	12	10.7	2409	21	10.5	3232	26	10.8	2219	30	11.6	2681	40	11.0	2339
11.0	1961	13	10.9	2286	22	10.4	3278	27	10.8	2247	31	11.6	2592	41	11.0	2273
11.0	2655	14	10.8	2390	23	10.3	3140				32	10.3	1975	42	10.8	2261
10.8	3072	15	10.4	2338							33	10.2	1984	43	10.8	2249
10.9	3081	16	10.5	2327							34	9.7	1712			
11.0	3758	17	10.5	2396							35	9.7	1758			
10.8	3770	18	10.2	2281							36	9.8	1767			
											37	9.0	1532			

by Akkermanns et al., [24] values greater than 5 are recommended to guarantee growth by pure coating.

Clearly, the modified *FN* for all the performed experiments (including those with a high percentage of agglomerates) are above 5, indicating that the minimum absolute value suggested by this theory is not directly applicable to the system under study. In addition, this approach does not provide a single value of the modified *FN* to estimate the condition for agglomerate formation. Indeed, the lower limit for the *FN* is dependent on the operating variables.

5.2. The dimensionless agglomeration parameter

Although the criteria available in the literature to predict the operating regimes were found to be valuable for other granulation systems, they cannot be directly applied to the urea melt granulation. For this reason, a new dimensionless agglomeration parameter (*DAP*) is postulated in order to univocally identify the growth regime. In fact, and as shown in Fig. 4, the dimensionless number N_{β_0} defined by Eq. (30) presents an univocous trend with the mass fraction of agglomerates. The presented data show that the mass fraction of agglomerates rises sharply for large N_{β_0} values. In fact, for $1/N_{\beta_0}<7$ the A (%) is higher than 5%, indicating that agglomeration is not negligible. However, although this dimensionless number correctly delimits the agglomeration and coating regions for the process under study, the calculation of N_{β_0} requires the PBE solution (i.e., it depends on the values of β_0 fitted from the given experimental data). Taking this into account and the need of having a parameter that depends only on the process conditions, Eq. (38) is rewritten as follows:

$$N_{\beta_0} = K\frac{\dot{m}_u{}^{1.5}\left(T_{fus}-T_{bed}\right)^{1.3}}{\dot{m}_{at}{}^{3.8}\left(u-u_{mf}\right)^{4.6}d_0{}^{2.3}} \tag{43}$$

where $\dot{m}_u = \dot{m}_L x_u$ and K represents:

$$K = 0.028\left[\frac{4\pi\rho_L d_{n,L} x_u \Delta H_{fus}{}^2 L}{9f(\theta)^2 cp_u k_p d_{n,g}\, m_{S0}}\right]^{0.3}\left[\frac{\left[x_u cp_u + (1-x_u)cp_w\right]}{x_u\Delta H_{fus}-(1-x_u)\Delta H_{ev}}\right]^{1.9} u_{mf}{}^{4.6}\left[10^6\frac{\pi d_{n,g}{}^2\mu_{at}}{4}\right]^{2.6} \tag{44}$$

For the case under study, K depends on variables that were not changed during the experiments; then, its value is constant and equal to 2.41×10^{-16} [(kg m/s^3)$^{2.3}$/°C$^{1.3}$]. Therefore, the new dimensionless agglomeration parameter *DAP* is defined as follows:

$$DAP = \frac{1}{N_{\beta_0}} = \frac{1}{K}\frac{\dot{m}_{at}{}^{3.8}\left(u-u_{mf}\right)^{4.6}d_0{}^{2.3}}{\dot{m}_u{}^{1.5}\left(T_{fus}-T_{bed}\right)^{1.3}} \tag{45}$$

It should be noted that the proposed parameter takes high values for low mass percentages of agglomerates (i.e., for pure coating as the predominant growth mechanism). Fig. 6 shows the experimental mass fraction of agglomerates as a function of the proposed parameter. Although N_{β_0} adequately represents the mass percentage of agglomerates for different operating conditions by a unique relationship (Fig. 4), the parameter *DAP* shows a higher dispersion (Fig. 6) since Eq. (45) does not involve the PBE solution and, thus, it does not comprise the best fitted β_0.

For a given maximum allowable limit of agglomerates in the final product, the appropiate *DAP* value can be easily set. For example, if the maximum acceptable value for the mass percentage of agglomerates is 5, *DAP* should be greater than 6 whatever the chosen combination of operating variables.

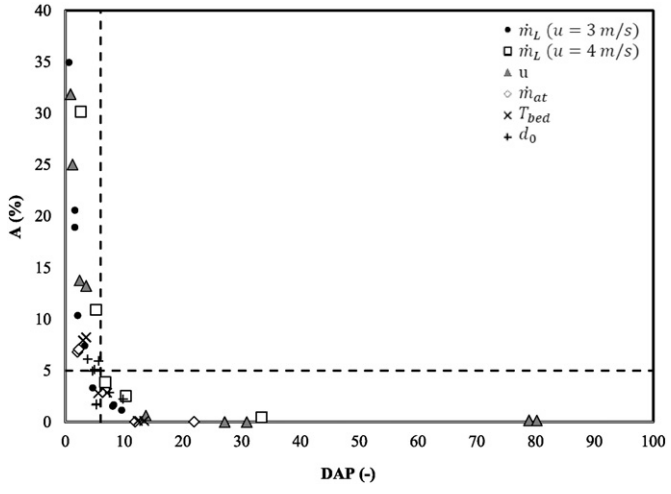

Fig. 6. Agglomerate mass percentage as a function of the dimensionless agglomeration parameter *DAP* for changes in different process conditions.

6. Conclusions

The population balance is the most frequently used modelling tool to describe a wide range of particulate processes. However, its application is limited by both the need of accurate kinetic parameters and appropriate numerical solution techniques. In an attempt to contribute to the modelling of fluidized-bed spray-on melt granulation systems, the urea granules production is particularly studied. For this specific process, which is carried out in a batch fluidized-bed unit where simultaneous coating and agglomeration occur, size-independent coating and agglomeration kinetics best describe the experimental data obtained under different melt and air atomization flowrates, air fluidization velocities, seed sizes and bed temperatures. Although the size of the colliding particles has no effect on the aggregation kernel, this parameter is strongly dependent on the process conditions. The correlation proposed to predict the SI kernel, from macroscopic variables and properties of the system, can be used to provide starting kernel factors for solving the PBEs governing spray-on melt granulation in fluidized-bed granulators.

Unlike criteria available in the open literature to predict the operating regimes for other granulation systems, the criterion proposed in this work adequately represents the spray-on urea melt fluidized-bed granulation. Besides, it is as a useful tool to select the process conditions that lead to the desired growth regime (coating or agglomeration). Further studies would be valuable to establish if the developed criterion can be used to predict the limit of agglomeration occurrence for other fluidized-bed spray-on melt granulation systems.

Acknowledgements

The authors want to thank Amel Khoufech and Khashayar Saleh (UTC, Compiegne, France) for their help to measure the urea restitution coefficient.

References

[1] H. Zhai, S. Li, D.S. Jones, G.M. Walker, G.P. Andrews, The effect of the binder size and viscosity on agglomerate growth in fluidised hot melt granulation, Chem. Eng. J. 164 (2–3) (Nov. 2010) 275–284.
[2] G.M. Walker, G. Andrews, D.S. Jones, Effect of process parameters on the melt granulation of pharmaceutical powders, Powder Technol. 165 (3) (Jul. 2006) 161–166.
[3] J.D. Osborne, R.P.J. Sochon, J.J. Cartwright, D.G. Doughty, M.J. Hounslow, A.D. Salman, Binder addition methods and binder distribution in high shear and fluidised bed granulation, Chem. Eng. Res. Des. 89 (5) (May 2011) 553–559.
[4] T. Abberger, A. Seo, T. Schaefer, The effect of droplet size and powder particle size on the mechanisms of nucleation and growth in fluid bed melt agglomeration, Int. J. Pharm. 249 (1–2) (Dec. 2002) 185–197.

[5] O. Maurstad, Population Balance Modeling of Agglomeration in Granulation Processes, Norwegian University of Science and Technology, 2002.
[6] R. Boerefijn, M.J. Hounslow, Studies of fluid bed granulation in an industrial R&D context, Chem. Eng. Sci. 60 (14) (Jul. 2005) 3879–3890.
[7] P.G. Smith, A.W. Nienow, Particle Growth Machanisms en Fluidised Bed Granulator-II, 1983.
[8] S. Iveson, J.D. Litster, K. Hapgood, B.J. Ennis, Nucleation, growth and breakage phenomena in agitated wet granulation processes: a review, Powder Technol. 117 (1–2) (Jun. 2001) 3–39.
[9] J. Litster, K. Hapgood, J. Michaels, A. Sims, M. Roberts, S. Kameneni, T. Hsu, Liquid distribution in wet granulation: dimensionless spray flux, Powder Technol. 114 (1–3) (Jan. 2001) 32–39.
[10] V. Pont, K. Saleh, D. Steinmetz, M. Hemati, Influence of the physicochemical properties on the growth of solid particles by granulation in fluidized bed, Powder Technol. 120 (1–2) (Oct. 2001) 97–104.
[11] M. Hemati, R. Cherif, K. Saleh, V. Pont, Fluidized bed coating and granulation: influence of process-related variables and physicochemical properties on the growth kinetics, Powder Technol. 130 (1–3) (Feb. 2003) 18–34.
[12] K. Saleh, D. Steinmetz, M. Hemati, Experimental study and modeling of fluidized bed coating and agglomeration, Powder Technol. 130 (2003) 116–123.
[13] F. Thielmann, M. Naderi, M.A. Ansari, F. Stepanek, The effect of primary particle surface energy on agglomeration rate in fluidised bed wet granulation, Powder Technol. 181 (2) (Feb. 2008) 160–168.
[14] A. Seo, P. Holm, T. Schaefer, Effects of droplet size and type of binder on the agglomerate growth mechanisms by melt agglomeration in a fluidised bed, Eur. J. Pharm. Sci. 16 (3) (Aug. 2002) 95–105.
[15] H.S. Tan, A.D. Salman, M.J. Hounslow, Kinetics of fluidised bed melt granulation I: the effect of process variables, Chem. Eng. Sci. 61 (5) (Mar. 2006) 1585–1601.
[16] S. Veliz Moraga, M.P. Villa, D.E. Bertín, I.M. Cotabarren, J. Piña, M. Pedernera, V. Bucalá, Fluidized-bed melt granulation: the effect of operating variables on process performance and granules properties, Powder Technol. 286 (2015) 654–667.
[17] D. Ramkrishna, Population Balances, Academic Press, London, England, 2000.
[18] A.A. Adetayo, B.J. Ennis, Unifying approach to modeling granule coalescence mechanisms, AICHE J. 43 (4) (1997) 927–934.
[19] N. Rao, Simulations for Modelling of Population Balance Equations of Particulate Processes Using Discrete Phase Model (DPM), Otto-von-Guericke- Universität Magdeburg, Magdeburg, Germany, 2009.
[20] R.H. Snow, T. Allen, B.J. Ennis, J.D. Litster, Size reduction and size enlargement, Perry's Manual 1999, pp. 20–23.
[21] K. Saleh, P. Guigon, Coating and encapsulation processes in powder technology, in: A.D. Salman, M.J. Hounslow, J.P.K. Seville (Eds.), Handbook of Powder Technology, Elsevier, Amsterdam, The Netherlands, 2007.
[22] D. Bertin, I. Cotabarren, J. Piña, V. Bucalá, Population balance discretization for growth, attrition, aggregation, breakage and nucleation, Comput. Chem. Eng. 84 (2016) 132–150.
[23] B.J. Ennis, G.I. Tardos, R. Pfeffer, A microlevel-based characterization of granulation phenomena, Powder Technol. 65 (1991) 257–272.
[24] J. H. M. Akkermans, M. F. Edwards, A. T. J. Groot, C. P. M. Montanus, R. W. J. Van Pomeren, and K. A. R. Yüregir, "Production of detergent granules," Patent WO98580461998.
[25] Production of granular urea as nitrogenous fertilizer, in: I.M. Cotabarren, D. Bertín, S. Veliz, L. Mirazú, J. Piña, V. Bucalá, C.M. Muñoz, A.M. Fernández (Eds.), Urea: Synthesis, Properties and Uses, NOVA Publishers 2012, pp. 1–63.
[26] T. Abberger, The effect of powder type, free moisture and deformation behaviour of granules on the kinetics of fluid-bed granulation, Eur. J. Pharm. Biopharm. 52 (3) (Nov. 2001) 327–336.
[27] I.T. Cameron, F.Y. Wang, C.D. Immanuel, F. Stepánek, Process systems modelling and applications in granulation: a review, Chem. Eng. Sci. 60 (14) (Jul. 2005) 3723–3750.
[28] J. Kumar, M. Peglow, G. Warnecke, S. Heinrich, L. Morl, Improved accuracy and convergence of discretized population balance for aggregation: the cell average technique, Chem. Eng. Sci. 61 (10) (May 2006) 3327–3342.
[29] J.D. Litster, B.J. Ennis, L. Liu, The Science and Engineering of Granulation Processes, Particle Technology Series, Kluwer Academic Publishers, Dordrecht, 2004.
[30] M. Catak, N. Bas, K. Cronin, S. O'Brien, E. Byrne, Mathematical modelling of a solid particle motion in a re-circulatory fluidised bed unit, Can. J. Chem. Eng. 89 (1) (2011) 92–100.
[31] M. Goldschmidt, Hydrodynamic Modelling of Fluidised Bed Spray Granulation, Twente University, 2001.
[32] M.J. Hounslow, The population balance as a tool for understanding particle rate processes, Kona 16 (16) (1998) 179–193.
[33] H.S. Tan, A.D. Salman, M.J. Hounslow, Kinetics of fluidised bed melt granulation, Powder Technol. 143–144 (Jun. 2004) 65–83.
[34] K.W. Chua, Y.T. Makkawi, B.N. Hewakandamby, M.J. Hounslow, Time scale analysis for fluidized bed melt granulation-II: binder spreading rate, Chem. Eng. Sci. 66 (3) (Feb. 2011) 327–335.
[35] K.W. Chua, Y.T. Makkawi, M.J. Hounslow, Time scale analysis for fluidized bed melt granulation III: binder solidification rate, Chem. Eng. Sci. 66 (3) (Feb. 2011) 336–341.
[36] H.S. Tan, A.D. Salman, M.J. Hounslow, Kinetics of fluidized bed melt granulation—II: modelling the net rate of growth, Chem. Eng. Sci. 61 (12) (Jun. 2006) 3930–3941.
[37] K.W. Chua, Y.T. Makkawi, M.J. Hounslow, Time scale analysis for fluidized bed melt granulation I: granule–granule and granule–droplet collision rates, Chem. Eng. Sci. 66 (3) (Feb. 2011) 318–326.
[38] D. Bertín, G. Mazza, J. Piña, V. Bucalá, Modeling of an industrial fluidized-bed granulator for urea production, Ind. Eng. Chem. Res. 46 (23) (Nov. 2007) 7667–7676.
[39] A. Clarke, T.D. Blake, K. Carruthers, A. Woodward, Surfaces, Langmuir 18 (8) (2002) 2980–2984.
[40] C.W. Visser, R. Pohl, C. Sun, G. Römer, B. Huis in't Veld, D. Lohse, Toward 3D printing of pure metals by laser-induced forward transfer, Adv. Maerials (September 2015).
[41] D. Bertin, I. Cotabarren, J. Piña, V. Bucalá, Population balance discretization for growth, attrition, aggregation, breakage and nucleation, Comput. Chem. Eng. 84 (2016) 132–150.
[42] H. Hu, S.A. Argyropoulos, Mathematical modelling of solidification and melting: a review, 4 (1996) 371–396.
[43] T. Jiménez, C. Turchiuli, E. Dumoulin, Particles agglomeration in a conical fluidized bed in relation with air temperature profiles, 61 (2006) 5954–5961.
[44] R.Y. Hong, Q.J. Guo, G.H. Luo, J. Zhang, J. Ding, On the jet penetration height in fluidized beds with two vertical jets, 133 (2003) 216–227.
[45] C.A. Chryssakis, D.N. Assanis, F.X. Tanner, Handbook of Atomization and Sprays, Springer, Canada, 2011.
[46] J.H. Meessen, Urea, Ullmanns Encyclopedia of Industrial Chemistry, John Wiley and Sons 2010, pp. 657–695.
[47] B.J. Ennis, G. Tarados, R. Pfeffer, A microlevel-based characterization of granulation phenomena, Powder Technology (1991).
[48] M. Wasserman, M. Ridyard, S. Capeci, W. Beimesch, and P. R. Mort, "Process for coating detergent granules in a fluidized bed," US6790821 B12000.
[49] P.D. Hede, P. Bach, A.D. Jensen, Validation of the flux number as scaling parameter for top-spray fluidised bed systems, Chem. Eng. Sci. 63 (3) (Feb. 2008) 815–828.
[50] R. Boerefijn, M. Orlovic, C. Reimers, M. Pogodda, M. Jacob, Application of the flux number approach for the simulation of granulation processes by use of flowsheeting tools, Chem. Eng. Sci. 86 (Feb. 2013) 137–145.
[51] A. Khoufech, M. Benali, K. Saleh, Influence of liquid formulation and impact conditions on the coating of hydrophobic surfaces, Powder Technol. 270 (2015) 599–611.
[52] F.P. Incropera, D.P. DeWitt, Fundamentos de Transferencia de Calor, México, Prentice Hall, 1999.
[53] D. Kunii, O. Levenspiel, Fluidization Engineering, Butterworth-Heinemann, Boston, 1991.